Iranian J Biotech. 2020 July;18(3): e2662 DOI: 10.30498/IJB.2020.2662

Research Article

# Enhancement of Pharmaceutical Urate Oxidase Thermostability by Rational Design of *De Novo* Disulfide Bridge

**Leila Rezaeian-Marjani[1], Mehdi Imani[1,2]*, Hossein Zarei Jaliani[3]**

[1] Department of Cellular and Molecular Biotechnology, Institute of Biotechnology, Urmia University, Urmia, Iran
[2] Department of Basic Sciences, Faculty of Veterinary Medicine, Urmia University, Urmia, Iran
[3] Department of Medical Biotechnology, School of Medicine, Shahid Sadoughi University of Medical Sciences, Yazd, Iran

**Corresponding author:* Mehdi Imani, Department of Basic Sciences, Faculty of Veterinary Medicine, Urmia University, Urmia, Iran.
Tel: +98-4431942618, Fax: +98-4432771926 E-mail: m.imani@urmia.ac.ir

**Background:** As a therapeutic enzyme, urate oxidase is utilized in the reduction of uric acid in various conditions such as gout or tumor syndrome lysis. However, even bearing kinetical advantage over other counterparts, it suffers from structural instability most likely due to its subcellular and fungal origin.

**Objectives:** In this research, by using rational design and introduction of *de novo* disulfide bridge in urate oxidase structure, we designed and created a thermostable urate oxidase for the first time.

**Materials and Methods:** Utilizing site-directed mutagenesis and only with one point mutation we constructed two separate mutants: Ala6Cys and Ser282Cys which covalently linked subunits of enzyme each other. Single mutation to cysteine created three inter-chain disulfide bridges and one hydrogen bond in Ala6Cys and two disulfide bridges in Ser282Cys.

**Results:** Both mutants showed 10 °C increase in optimum activity compared to wild-type enzyme while the $K_m$ values for both increased by 50% and their specific activity compromised. The thermal stability of Ser282Cys increased remarkably by comparing Ala6Cys and wild-type enzymes. Estimation of half life for wild-type enzyme demonstrated 38.5 min, while for Ala6Cys and Ser282Cys were 138 and 115 min, respectively. Interestingly, the optimal pH of both mutants was broaden from 7 to 10, which could make them candidates for industrial applications.

**Conclusion:** It seemed that introducing disulfide bridges resulted in local and overall rigidity by bringing two adjacent sites of enzyme together and decreasing the conformational entropy of unfolding state is responsible for the enhancement of thermostability.

***Keywords:*** Aspergillus flavus, Disulfide bridge, Gout, Site-directed mutagenesis, Urate oxidase

## 1. Background

A final product of purine catabolism, uric acid in human and primates is normally excreted in urine. It has been proved that the normal range of uric acid concentration in human serum is 1.5 to 6.0 mg.dL$^{-1}$ in women and 2.5 to 7.0 mg.dL$^{-1}$ in men (1). Due to low water-solubility of uric acid, any overproduction of uric acid or failure in its excretion via kidney leads to hyperuricemia and formation of crystals of uric acid in the form of monosodium urate. Moreover, gout, tumor lysis syndrome (TLS) (2), chronic kidney disease are known to be involved in the development of hyperuricemia, as well. In all organisms, a functional enzyme called uricase (urate oxidase) is available whose role is conversion of water-insoluble uric acid to water- soluble and readily-excreted allantoin except in primates, birds, and some species of reptiles which have loosen their respective enzyme during evolution of their genome. Human uricase has also followed this evolutionary path and has been subsequently disabled (3). For the treatment of hyperuricemia, allopurinol and febuxostat, two competitive inhibitors of xanthine oxidase restraining uric acid production. They do not reduce accumulated uric acid but its production. Nonetheless, they are not able to prevent refractory gout which occurs in patients suffering from sensitivity to allopurinol and febuxostat (4).

Recently, uricolytic therapy with uricase has been

developed for treatment of gout disease which has advantage over allopurinol and febuxostat therapy in which accumulated uric acid crystals decompose to easily-excreted allantoin (5, 6). Rasburicase and pegloticase are two uricases for reduction of uric acid in hyperuricemia condition. Raburicase is a brand name for a recombinant *Aspergillus flavus* uricase which was approved for primary treatment of TLS while pegloticase is applied for treatment of chronic gout and patients who are resistant too conventional therapy (7). *Aspergillus flavus* urate oxidase (UOX) contains 302 amino acids with the molecular weight of 34.2 kDa. The enzyme is a globular homotetramer with total mass of 135 kDa (8-10). Molecular cloning of *Aspergillus flavus* UOX gene was performed in 1992 (11). However it has been cloned, expressed and studied by different research groups (11-15).

Enhancement enzymes and proteins stability is of great interest. Generation of weak interactions such as hydrogen bond, replacement of glycine with other amino acids, hydrophobic interactions (16), introduction of proline residues, immobilization, and introduction of disulfide bridges are common strategies to fulfill this goal. Among them, disulfide engineering is one of the effective strategies for enhancing protein thermostability. Although not success in all attempts, but in most cases insertion of de novo disulfide bridge increases enzyme and protein thermal stability (17).

## 2. Objective

Engineering of urate oxidases either rational or random designs were only limited to a few works (18). However, no disulfide bridge engineered in uricase except for *Bacillus* sp. TB-90 urate oxidase which was implemented by Hibi group in 2016 (19). Surveying the protein sequence and 3-D structure of uricase showed that there are only three cysteine residues in each monomer at positions 35, 103 and 290 neither of which has ability in disulfide bridge formation in wild-type form. However, generation of disulfide bridge in *Aspergillus flavus* uricase has not been reported yet. Therefore, the current research aimed to design and create *de novo* disulfide bridge in *Aspergillus flavus* uricase to create an improved enzyme using site-directed mutagenesis technique.

## 3. Materials and Methods

### *3.1. Materials*

Uric acids sodium salt (U2875) and 5,5′-ditio-bis 2-nitrobenzoic acid (DTNB) were obtained from Sigma-Aldrich. *Restriction enzymes*, T4 DNA ligase, and isopropyl-b-D-thiogalactopyranoside (*IPTG*) was obtained from Fermentas. Plasmid extraction kit, gel purification kit, were obtained from Bioneer Corp. $Ni^{2+}$-NTA agarose (30210**)** was from Qiagen. Bacterial culture medium was from Scharlau company. SDS-PAGE kit and protein assay kit were from Arsam Fara Zist Corp., Iran.

### *3.2. Microorganisms*

All *E. coli* cells were obtained from Pasteur institute of Iran except for Shuffle. Suitable for expression of disulfide bridge-containing protein *E. coli* strain, SHuffle®, was purchased from New England Biolabs, Inc. A parental plasmid containing bacterial codon-optimized synthetic coding sequence of *Aspergillus flavus* uricase which was already cloned into pET-28a(+)(20), was used for site-directed mutagenesis.

### *3.3. Computer Modeling*

Crystal structure of *Aspergillus flavus* uricase (PDB: 1xxj) was used as a model for screening proper location of cysteine residues for generation of stabilizing disulfide bridges using *in silico* analysis provided by National Center for Biological Sciences Server (NCBS-IWS) (http://caps.ncbs.res.in/iws/modip.html) and rechecked by (http://cptweb.cpt.wayne.edu/DbD2) (21-23). For visualization of 3D structure of wild-type and modeled enzymes, Swiss-PDB Viewer application was utilized.

### *3.4. Site-Directed Mutagenesis*

Splicing by Overlap Extension (SOE) and conventional PCR were carried out to alter the codon of selected amino acids to cysteine codons on the plasmid *pET-28a* containing gene of *Aspergillus flavus* uricase. Site-directed mutagenesis by SOE PCR includes incorporation of mutagenic primers in independent PCRs and eventually combining the two fragments in the second PCR. The reaction carried out with flanking primers (A and D) which matching to the both sides of the uricase sequence, and two internal mutated primers (bearing codon of cysteine) (B and C) with complementary ends which are essential for second PCR. Then, the amplified fragments of AB and CD are mixed and PCR launched using primers A and D (**Table 1**). Once the whole part of gene amplified which contains the mutated internal sequence, goes under restriction enzyme digestion and is incorporated into desired plasmid (24). Practically, for creating mutant Ser282Cys, we utilized SOE PCR whereas for Ala6Cys/Cys290 a regular PCR reaction was applied.

For amplification of fragments AB and CD of SOE

PCR, 1 µL of the plasmid containing synthetic *Aspergillus flavus* uricase gene was employed as a template. The PCR cycling program was as follows: the initial denaturation at 94 ºC for 5 minutes, a 30 cycle (94 ºC for 1 minute, 55 ºC for 1 minutes, and 72 ºC for 3 minutes), and the final cycle was followed by extension at 72 ºC for 10 minutes. The expected amplicon size for fragments AB and CD were 1161 and 427 bp, respectively. Once the fragments are visualized on agarose gel 1% and purified, they were mixed in 1:1 ration and used as a template for third PCR. The final amplification was implemented by a two-step PCR: the first step was carried out 15 cycles followed by adding primers A and D and continued 30 more cycles in the second step under the following program: initial denaturation at 94 ºC for 1 minutes, a 30 cycle (94 ºC for 1 minutes, 55 °C for 1 minutes, and 72 ºC for 4 minutes), and the final extension was performed for 10 minutes at 72 ºC. The resulting mutant (AD fragment) with size of 1568 bp went under the digestion with *NcoI* and *XhoI*, inserted into *pET-28a(+)*by T4 DNA ligase and followed by chemical transformation into competent cells of *E. coli* strain, *SHuffle®*.

### *3.5. Verification of Cloning*

In order to confirm the cloning of PCR products into *pET-28a(+)* five positive colonies randomly selected, grown in LB medium, and miniprepped for plasmid minipreparation. Colony PCR was performed using *pET-28a(+)*-specific oligonucleotides (**Table 1**). Finally, mutant plasmids were sequenced by ABI 3730XL DNA Analyzer (*Bioneer Sequencing* Service).

### *3.6. Enzymes Expression and Purification*

10 mL of LB medium containing 50 µg.mL$^{-1}$ of kanamycin was inoculated with a single colony and grown at 37 °C overnight with vigorous shaking. Then, 2 mL of overnight culture was transferred to 200 mL of LB media and shaked vigorously at 37 °C until the OD of 0.6-0.7 was achieved. The protein induction was implemented by IPTG 1 mM followed by incubation at 28 °C for 12 hours. Afterwards, bacteria expressing UOX and mutant enzymes were collected and re-suspended in tris-based lysis buffer pH 7.4 (contained NaCl 300 mM and imidazole 5 mM), and sonicatedon ice water bath. Finally, recombinant wild-type and mutant enzymes were purified by Ni-NTA column. Briefly, the column was pre-equilibrated with 3 column volumes of lysis buffer. The cells supernatant then was loaded on the pre-equilibrated column. Next, after washing the column with wash buffer the enzymes were eluted by using elution buffer (Tris buffer pH 7.4 containing 300 mM imidazole). Eventually, the purified enzymes run on the SDS-PAGE 12.5% for purity analysis. In each step, protein quantity was estimated based on Bradford method (25).

### *3.7. SH-Group Titration*

In order to assess the disulfide bridge formation the quantity of thiol groups was titrated using Ellman's reagent (26). The enzymes went under non-reducing and denaturing conditions using urea and temperature and their SH group quantified. The reaction condition was as follows: protein 2.5 µM, DTNB, 1 mM and urea 6M. The denaturation time for enzymes was 20 min before adding DTNB. The release of TNB anions

**Table 1** Oligonucleotides used in this study. Underlined and lowercases bases are substitutions. Underlined bases in bold font are overlapped bases in second PCR.

| **Oligonucleotides for S282C (AGT to TGC)** | **sequences** |
|---|---|
| A (*pET-28a* body) | F: 5′-TGCATGCAAGGAGATGGCGCCCAAC -3′ |
| B (mutant) | R: 5′-CCGTTCGGATC**gca**TTGGGGCGCAAAGACCTC -3′ |
| C (mutant) | F: 5′-CCCCAA**tgc**GATCCGAACGGTCTG-3′ |
| D (*pET-28a* body) | R: 5′-AAAGGGAGCCCCCGATTTAGAGC-3′ |
| BC fragments hybridization | 5' **CCGTTCGGATCGCATTG**GGGCGCAAAGACCTC 3'<br>3' GTCT**GGCAAGCCTAGCGTAAC**CCC 5' |
| Oligonucleotides for A6C **GCG to TGC** | sequences |
| F (mutant) | F: 5′-AAGGAGCCATGGCAGCCGTGAAGGCA**tgc**CGCTATGGTAAAGAC-3′ |
| R (*pET-28a* body) | R: 5′-AAAGGGAGCCCCCGATTTAGAGC-3′ |

as a result of DTNB reaction with free SH groups were spectrophotometrically measured at 412 nm. For calculation of thiol numbers, the extinction coefficient of 14.15 $mM^{-1}cm^{-1}$ for TNB was considered. For enzymes molarity estimation, the molecular weight tetramer assemble, 135 kDa, was considered.

*3.8. Wild-Type and Mutant Uricases Assay*

For uricase enzyme assay, decomposition of uric acid to allantoin was spectrophotometrically followed at the wavelength of 293 nm. 20 µL of UOX enzyme was added to the reaction buffer containing boric acid buffer (20 mM pH 8.5), and 20 µL of 48 µM uric acid. The enzyme reaction terminated in 6 minutes and reduction in absorbance of uric acid was measured at 293 nm. One unit of uricase activity was defined as the amount of enzyme that catalyzes the catalysis of 1µM uric acid to allantoin per minute at pH 8.5 (13, 27, 28). Enzyme activity was determined based on the following equation:

$$\mathrm{U/ml} = \frac{(\Delta A_{293}/\min \mathrm{Test} - \Delta A_{293}/\min \mathrm{Blank})(\mathrm{df})}{12.6 \times 0.02}$$

Whereas,
df = Dilution factor
12.6 = Millimolar extinction coefficient of Uric Acid at 293nm
0.02 = Volume of enzyme (mL)

*3.9. Enzymes Characterization*

*3.9.1. pH Profile Assessment*

To obtain the pH profile of wild-type and mutant enzymes, their activities were assessed in the range of pH 3.0 to 12. To prepare buffer for wide pH range a mixture of three buffer including citrate, phosphate and tris was used.

*3.9.2. Optimum Temperature*

To identify the optimum temperature of enzymes, their activities were assayed after pre-incubation in each desired temperature from 5 to 60 °C for 6 minutes. 20 µL of enzymes added to the pre-heated substrate cocktail and assayed by following conversion of uric acid to allantoin, spectrophotometrically.

*3.9.3. Thermal Inactivation and Stability Assays*

To assess thermal inactivation, purified enzymes incubated in temperature range of 0 to 60 °C for 6 minutes and then placed on ice for 20 minutes for renaturation. Afterwards, the enzymes residual activities were determined at room temperature by recording absorbance at 293 nm. To estimate enzyme inactivation rate constant ($k_{in}$) the Ln of enzyme activity plotted against time and the slope ($-k_{in}$) was determined. The half-life ($t_{1/2}$) of the activity which is the indicator of 50% loss of enzyme initial activity calculated using $t_{1/2} = 0.693/k_{in}$.

For thermal stability studies, appropriate amount of enzymes were incubated at 40 °C for 60 minutes and aliquots of 20 µL were removed at a given time period (5 minutes), and chilled on ice for 30 minutes and assayed.

*3.10. Statistical Analysis*

Each experiment was repeated three times in an independent manner (n=3). To analyze the significance of difference between the results student's t-test was used. All data were expressed as mean±SD. Significance of $P< 0.05$ has been given receptive in all test.

## 4. Results

*4.1. Selection of Mutation Sites*

To discover the potential cysteine mutation locations on uricase, the crystal structure of *Aspergillus flavus* uricase (PDB: 1xxj) was uploaded to the NCBS Integrated Web Server. Applying stereochemical parameters such as the distances between two $C^{\alpha}$, two $C^{\beta}$, and two sulphur atoms of two neighboring amino acids, side chain torsion angles $\chi_{ss}(C^{\beta}\text{-}S^{\gamma}\text{-}S^{\gamma}\text{-}C^{\beta})$, $\chi_1(N\text{-}C^{\alpha}\text{-}C^{\beta}\text{-}S^{\gamma})$, and $\chi_2(C^{\alpha}\text{-}C^{\beta}\text{-}S^{\gamma}\text{-}S^{\delta})$ surface accessibility, residue depth and B-factor, the server predicts the correct mutation site (17, 29). The modeling results offered 400 pairs but only 33 of modeled fall into grade A which indicates the higher probability of disulfide bridge formation. Eventually, we chose only 2 points considering critical amino acids essential for enzyme conformation and reaction catalysis maintenance which were excluded from our selection.

The selected points include Ala 6 and Ser 282 which mutating them to Cys would connect position 6 with enzyme's own Cys 290 from opposite subunit together and position 282 of each subunit with opposite one together, as shown **Table 2**. As well as server prediction, the disulfide bridges formation probability was examined by Swiss-PDB Viewer (**Fig. 1**).

*4.2. Correct Formation of Engineered Disulfide Bridges*

Once the gene mutated by site-directed mutagenesis and cloning the cloned mutant enzyme gene confirmed by sequencing (**Fig. 2**). In order to express mutant enzymes *E. coli* strain SHuffle® which is a convenient strain for production of disulfide-containing proteins,

**Table 2** Description of the designed disulfide bond and their location on the enzyme. The capital letters in last column indicate the chain number of urate oxidase.

| Mutant names | positions | Number of linkages | Disulfide linkage between chains positions |
|---|---|---|---|
| **A6C/C290** | Ala 6 | 3 SS and 1 H-bond | A6-B290, A290-B6, C6-D290 and C290-D6 |
| **S282C/S282C** | Ser 282 | 2 | A-D and B-C |

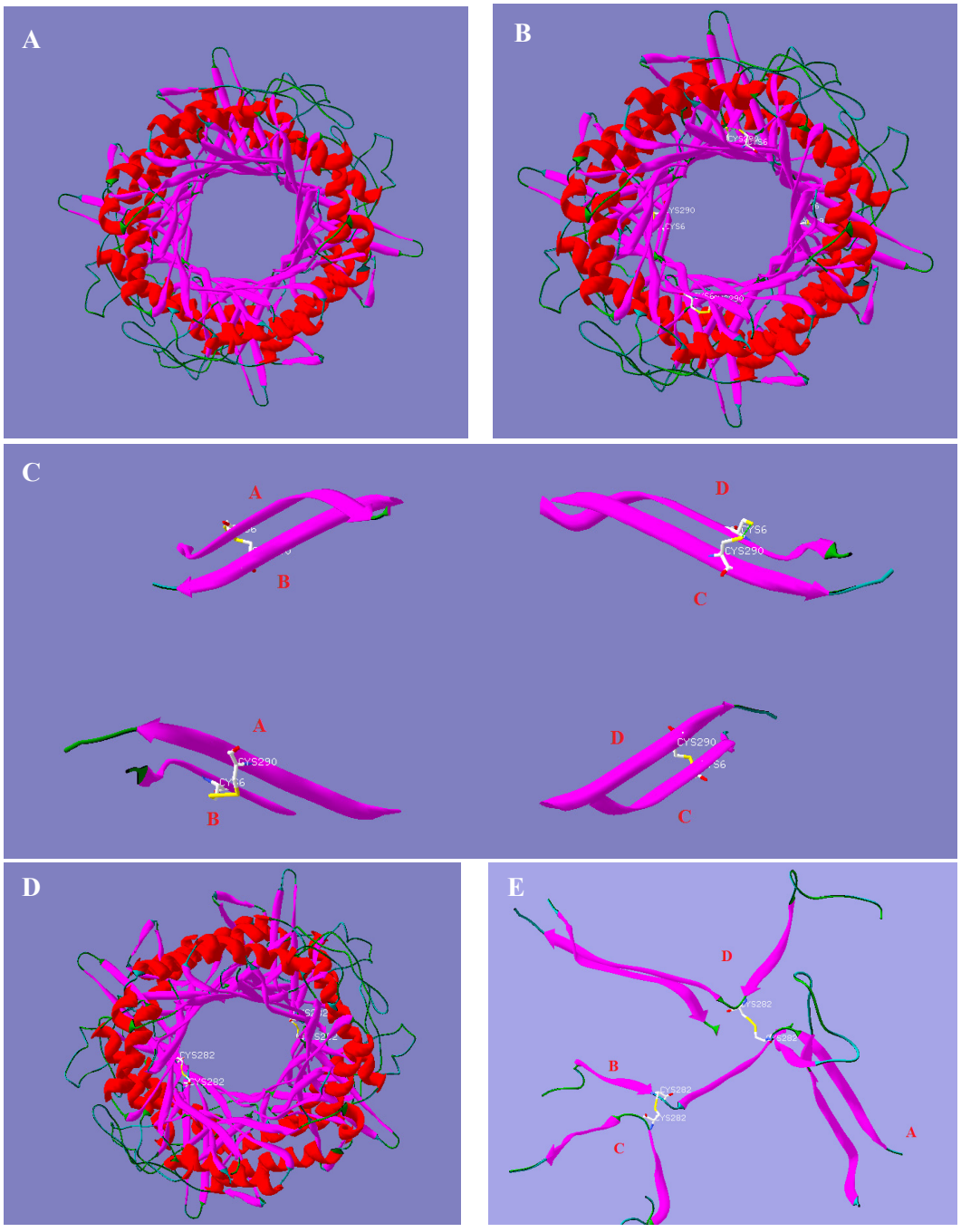


**Figure 1.** 3D structure of urate oxidase and modeled mutants. All structures were constructed by Swiss-PDB Viewer and PDB 1xxj was used as a template for modeling. (A) Full and top view of tetrameric wild-type urate oxidase. (B) Full view of Ala6Cys mutant with four mutated spots. (C) The structure B with removed residues except for those involved in new disulfide and hydrogen bonds formation. (D) Full and top view of mutant Ser282Cys with two new disulfide bonds spots. (E) Details of two disulfide bonds in mutant Ser282Cys. The capital letters show the monomers.

was employed to reach mutant enzymes with disulfide bridge formation. Although, the mismatched formation of disulfide between free cysteines, and as a result, protein aggregation is very likely during protein expression, the presence of mutant enzymes activity implies the lack of disulfide mis-formation. However, to confirm disulfide bridge formation titration of free SH group by DTNB reagent was performed (23). As shown in **Table 3** the amount of free -SH of wild-type and mutant enzymes in the native state is roughly three. While incubation of three enzymes with urea 6 M and DTNB revealed approximately 12, 9, and 12 for wild-type, Ala6Cys and Ser282Cys, respectively.

*4.3. Kinetic Properties Urate Oxidases*

To address the impacts of disulfide bridges on the kinetic attributes of the enzymes, optimum temperature, relative specific activity, $K_m$,$V_{max}$, $K_{cat}$, and optimum pH were measured. The optimum temperature of both mutants increased 10 °C compared to native urate oxidase which was 25 °C. Assessment of relative specific activity showed nearly a 50% decrease for both mutants in comparison to wild type enzyme. Evaluation of $K_m$ for uric acid of both mutants exhibited an increase by 20% and 30% for Ala6Cys and Ser282Cys, respectively and $V_{max}$ for Ala6Cys decreased by 12%, but that of Ser282Cys

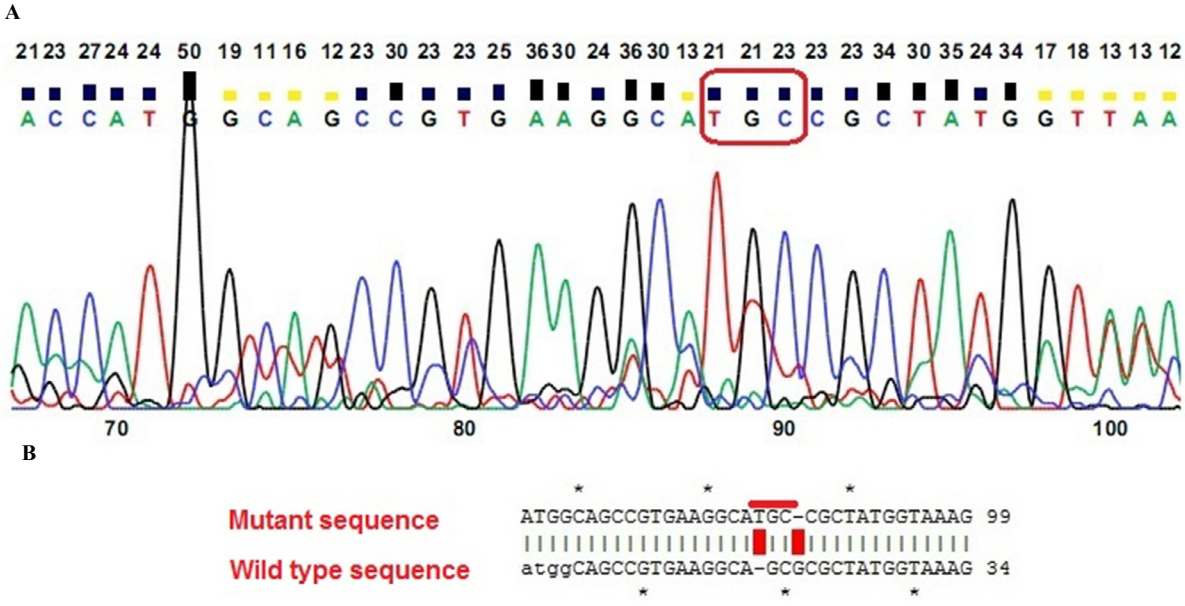


**Figure 2.** (A) DNA sequencing chromatogram of Ala6Cys mutant in which the substituted nucleotides are indicated in red rectangle. (B) Alignment of wild type sequence with mutated one where mismatch point implies the mutation points.

**Table 3** Titration and quantification of thiol groups in urate oxidase and its mutants. Numbers are represented in mean ± SD.

| | TNB (mM) | Enzyme (mM) | Free thiol/ native enzymes (mole/mole) | Free thiol/ denatured enzymes (mole/mole) |
|---|---|---|---|---|
| UOX | 0.010 | 0.0037 | 2.86±0.76 | 11.46±1.13 |
| Ala6Cys | 0.011 | 0.0037 | 2.97±0.57 | 9.73±0.79 |
| Ser282Cys | 0.011 | 0.0037 | 3.12±1.08 | 12.44±0.78 |

**Table 4** Kinetic characterization of wild type urate oxidase and its mutants.

| | Optimum temperature (°C) | Relative specific activity | $K_m$ (µM) | $V_{max}$ (U) | $K_{cat}$=TON (1/sec) | Optimum pH | Half-life (min) |
|---|---|---|---|---|---|---|---|
| UOX | 25 | 100 | 79.7 | 7 | 15.76 | 8.5 | 43 |
| Ala6Cys | 35 | 53.85 | 94.04 | 6.2 | 19.14 | 8 | 138 |
| Ser282Cys | 35 | 52.24 | 104.8 | 8.5 | 13.96 | 8.5 | 115 |

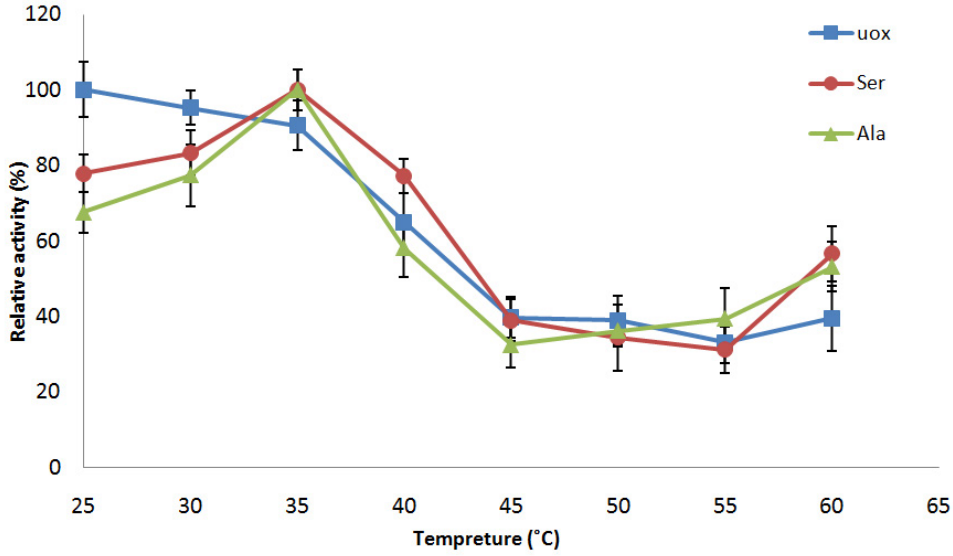


**Figure 3.** Thermal inactivation of wild type urate oxidase and its mutants. The remaining activity was expressed as a percentage of maximum activity. (■) urate oxidase, (▲) mutant Ala6Cys, and (●) mutant Ser282Cys. Each value represents the mean of three independent experiments, and the error bars are based on the standard of mean.

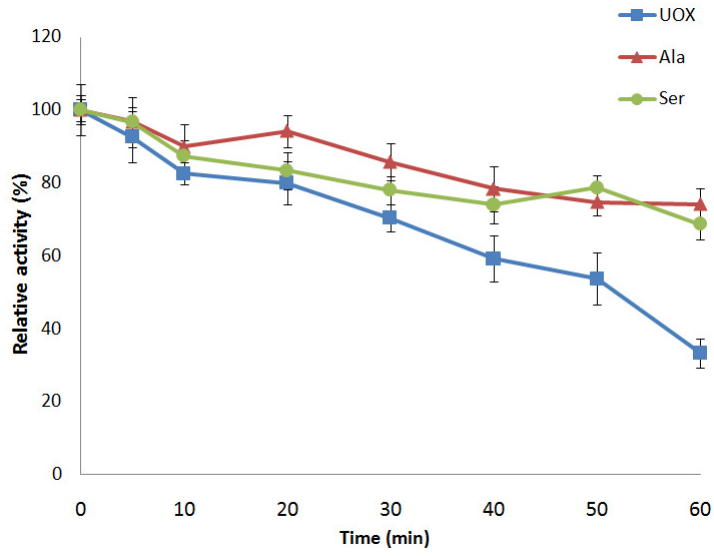


**Figure 4.** Thermal inactivation of wild type urate oxidase and its mutants. (■) urate oxidase, (▲) mutant Ala6Cys and, and (●) mutant Ser282Cys. Each value represents the mean of three independent experiments, and the error bars are based on the standard of mean.

increased by 20%. Estimation of turn over number for both mutants indicated 19 and 14 ($sec^{-1}$) for Ala6/Cys and Ser282Cys, respectively (**Table 4**). The optimum pH value did not show any significant changes, rather than for Ala6Cys mutant that displayed a decrease from 8.5 to 8 (**Table 4**). It is worthwhile to mention that even though the pH 8 considered optimum for mutant Ala6Cys, but its activity broadens from pH 6 to 10 relative to mutant Ser282Cys and wild-type enzyme (data is not shown).

*4.4. Thermal Inactivation and Stability Measurements*

Thermal inactivation of native and mutant enzymes was performed by following their activities at different temperatures. The results revealed that the activity of Ala6Cys and Ser282Cys declined approximately to 60% and 77% of initial activities after incubation at 40 °C for 6 minutes, respectively, whereas for the native uricase remained 65% (**Fig. 3**).

Examination the thermal stability of enzymes at 40 °C as a function of time showed that Ala6Cys and Ser282Cys

remained almost 75% and 70% of their initial activity, respectively, while the remaining activity of wild-type enzyme was nearly 35% over 60 minutes (**Fig. 4**). Evaluation of $k_{in}$ demonstrated that urate oxidase $k_{in}$ is almost 0.016 $min^{-1}$ whereas it is declined to 0.005 and 0.006 $min^{-1}$ for Ala6Cys and Ser282Cys, respectively. Estimation the half-life for wild type and mutant enzymes indicated that replacement of Ala6 and Ser282 with Cys enhanced urate oxidase half-life from 43 minutes to 138 and 115 minutes, respectively (Table 4).

## 5. Discussion

Designing and introducing disulfide bridges in proteins structure to enhance their thermostability is a common strategy in protein engineering (30). The enzyme urate oxidase which involved in degradation of final product of purine nucleotides degradation is absent in primates, birds and some reptiles species for evolutionary reasons (18). Bearing favorable characteristics such as kinetic features, and partial thermostability, *Aspergillus flavus* has gained a remarkable attention for clinical application.

To improve thermostbility and develop a new improved enzyme, we rationally designed and introduced *de novo* disulfide bridges in urate oxidase for the first time using site-directed mutagenesis technique and investigated its kinetic traits.

In addition to modeling servers which gave us 400 predicted models, the critical amino acids which were essential for enzyme catalytic activity and conformational stability were carefully considered to be conserved. The conserved amino acids positioned within the active site assumed possible residues in conservation of conformation and function of the enzyme were excluded from the selection (8).

Therefore, two points Ala 6 and Ser 282 were selected to be mutated separately. The Ala 6 residue is located in the β-strand secondary of enzyme and it is predicted that once it is mutated to cysteine it would form disulfide bridge with Cys 290 of opposite chains of enzyme. Hence, the A6C/C290 mutant conveys 3 disulfide bridge and one hydrogen bond. Moreover, mutating of other selected point, Ser 282, to Cys would connect the subunits of A to D and B to C. Interestingly, Ser 282 is located in loop region and hence connects two flexible area of protein together (**Table 2**). Before getting started, the possibility of disulfide bond formation was examined by Swiss-PDB Viewer (**Fig. 1)**.

Once mutagenesis was implemented and confirmed by sequencing, the mutant urate oxidases were expressed in *E. coli* strain SHuffle® which is an engineered strain for production of disulfide-containing proteins. Moreover, while mismatched and scrambled formation of disulfide between free cysteines results in protein aggregation and hence enzyme dysfunction, observation of enzymes activity can be considered as a sign of disulfide bridge correct formation. Additionally, non-enzymatic nature of disulfide bridge formation makes it a spontaneous reaction. Furthermore, proper dislulfide bridge formation in proteins with high number of disulfide bridge such as mouse urokinase with six, and human tissue plasminogen activator (tPA) with 17 disulfide bridges in engineered *E. coli* strains with oxidative cytosol adapt *E. coli* suitable host for disulfide-bearing protein (31, 32). However, regardless of those, to confirm disulfide bridge formation free thiol titration by DTNB reagent was performed (23) As results showed, the amount of free -SH of wild-type and mutant enzymes in the native state is roughly three which can be attributed to the accessible thiol groups. While thiol titration in denatured condition revealed approximately 12, 9, and 12 for wild-type, Ala6Cys and Ser282Cys, respectively. These results implied that the engineered Cyc residues involved in disulfide bridge formation rather than standing free thiol.

Kinetic characterization of wild type and mutant enzymes indicated that optimum temperature for the wild type enzyme was 25 °C which was in compatible with previous studies (20) while for both Ala6Cys and Ser282Cys mutants it increased by 10°C. Investigation pH profile at different pH range (pH 3-13) showed the same optimum pH for all three enzymes (pH 8.5). Estimation of relative specific activity showed a 50 % decline for both mutants relative to wild type one. Decrease of specific activity upon disulfide introduction was also evident in other studies (17). Significant increase in $K_m$ for both mutant enzymes relative to wild type urate oxidase could explain the reduction of relative specific activity which can be explained by the fact that mutant enzymes affinity for uric acid declined leading to enzyme activity reduction. Moreover, cross-linking two regions of a protein by disulfide bridge impose rigidity to protein conformation suggesting loss of mutant enzymes conformational flexibility in absorbing uric acid. It can also be explained that the mutations might affect the protein dynamics and therefore the catalysis conciliated.

To analyze further enzymes characteristics, thermal inactivation and thermal stability experiments were conducted. Measurement of thermal inactivation indicated that wild type enzyme and Ala6Cys mutant lost approximately 40% of initial activity after incubation at 40 °C for 6 minutes while Ser282Cys did only 25% (Fig. 3). To further assess the kinetic stability,

all enzymes were incubated at 40 °C in the course of time. The measurements indicated that 35% of wild type enzyme activity was preserved after 60 minutes. By contrast, 70% of initial activities of both mutant enzymes were remained after 60-minute incubation at 40 °C suggesting higher resistance of mutant enzymes against heat inactivation in comparison to wild type one. Even tough, thermal inactivation analysis of Ala6Cys showed drop in activity relative to wild type but thermal stability experiments showed that it can stand heat longer time comparing wild type enzyme. For Ser282Cys both thermal inactivation and stability experiments proved improvement relative to other two enzymes.

Stabilization of urate oxidase by disulfide bridge can be either attributed to resistant against heat denaturation or refolding of enzyme after cooling on ice. In either way, the protective effect of disulfide on urate oxidase would help the enzyme to tolerate harsh denaturing conditions. Assessment of half-life as a further criterion for enzyme kinetic stability at 40 °C showed that Ala6Cys enhanced the half-life of enzyme 3.2 fold, whereas Ser282Cys had 2.6 fold improved half-life (Table 4). Moreover, evaluation of thermal inactivation rate constant, $k_{in}$ showed that the Ala6Cys and Ser282Cys $k_{in}$ were 31% and 37% of that of wild type enzyme which indicates a milder trend of thermal inactivation relative to wild type enzyme. The results of thermal stability experiments imply that disulfide bridge in both mutants endow the enzyme, an ability against heat and hence delay in thermal denaturation.

By mutating Ala 6 residue to Cys, it is in convenient position to form disulfide bridge with corresponding opposite monomer of urate oxidase. The three disulfide bridges formed between position 6 of monomer A with position 290, position 290 of monomer A with position 6 of monomer B, and position 6 of monomer C with position 290 of monomer D. Additionally, one new hydrogen bond induced after mutating Ala 6 to Cys between monomer C and D in position 290 and 6 (**Fig. 2**). It can be postulated that the generation of disulfide bonds and new hydrogen bonds between monomers resulted in both local and total rigidification of the urate oxidase hence improved thermostability. In the case of mutant Ser282Cys, mutating Ser282 to Cys induced two inter chain disulfide bridges between monomers A and B, and C and D which cross-linked two monomers of urate oxidase each other.

The mechanism proposed for enhancement of protein stabilization by generation of new disulfide bridges include lowering the entropy of unfolded state and decrease of unfolding rate of denatured protein (33). Several researches demonstrated that any reinforcement in protein tertiary structure by development of physico-chemical interactions such as hydrogen bonds (34), hydrophobic and electrostatic interactions and disulfide bridge enhance thermodynamic stability of protein which normally give rise to kinetic stability in case of enzymes (35, 36).

Due to the lack of sufficient data, one cannot explicitly offer thermal instability mechanism for uricase. However, it can be attributed to tertiary and quaternary structure labiality against environmental condition. Additionally, it is demonstrated that pushing equilibrium of protein folding reaction [unfolded (U) <⟶> native (N)] toward N state can stabilize the protein structure. Presence of disulfide bridge in a protein destabilizing U state by lowering the entropy of unfolded state favors N state. This mechanism can be applied to our mutants in which newly-introduced disulfide bridges decrease the entropy of urate oxidase unfolded state and maintain the enzyme in native state. This is the reason why the mutants showed remarkable resistance against unfolding in comparison to wild type enzyme. Based on the value of half-life of mutant enzymes and wild-type it is evident that mutant enzymes are more thermostable than wild-type one.

Since protein stabilization by generation of new disulfide bridge is one of the most effective strategies in enhancement of protein stability, the results of our study showed that though mild reduction and compromising in the kinetic activity of both mutants were inevitable but enhanced thermal stability endowed the enzyme a characteristic in which it could overcome heat labiality at longer times of exposure.

## 6. Conclusions

Thermostabilization of urate oxidase is essential for its half-life in the therapeutic and industrial application. In this research, we designed and introduced *de novo* disulfide bridge to naturally disulfide-free enzyme in order to improve its thermostability. Two created mutants showed remarkable thermostability and higher optimum temperature, but losing half activity in comparison to wild-type enzyme was the main drawback. Although the activity of the mutant enzyme was negatively compromised, but new traits empower the enzyme to tolerate harsh reaction conditions.

Collectively, we speculate that generation of disulfide bridge in urate oxidase stabilized its structure most probably by restricting the flexibility and rigidification. Moreover, enhanced stability and half-life of engineered urate oxidase suggest reduced therapeutic and industrial doses as well as longer storage lifetime for uricase.

Eventually, considering its thermal stability, Ser282Cys is suggested for therapeutic and industrial applications despite more details of structural analysis are essential.

## Conflict of interest statement

The authors declare that there is no conflict of financial interests.

## Acknowledgement

This research has been financially supported by research council of Urmia University. Mr. Ashkan Basirnia and Mrs. Razieh Pak-Tarmani is highly appreciated for their kind cooperation, as well.

## References

1. Maiuolo J, Oppedisano F, Gratteri S, Muscoli C, Mollace V. Regulation of uric acid metabolism and excretion. *Int J Cardiol.* **2016; 213**:8-14. doi: 10.1016/j.ijcard.2015.08.109.
2. Cheuk DKL, Chiang AKS, Chan GCF, Ha SY. Urate oxidase for the prevention and treatment of tumour lysis syndrome in children with cancer. *Cochrane Database of Systematic Reviews*. **2017**(3). doi: 10.1002/14651858.CD006945.pub4.
3. Chang BSW. Ancient insights into uric acid metabolism in primates. *Proc Natl Acad Sci.* **2014;111**(10):3657-8. doi: 10.1073/pnas.1401037111.
4. Yang X, Yuan Y, Zhan C-G, Liao F. Uricases as Therapeutic Agents to Treat Refractory Gout: Current States and Future Directions. *Drug Dev Res.* **2012;73**(2):66-72. doi: 10.1002/ddr.20493.
5. Nuki G. Chapter 14 - Uricase Therapy of Gout A2 - Terkeltaub, Robert. Gout & Other Crystal Arthropathies. Philadelphia: W.B. Saunders; **2012**. p. 174-86.
6. Alakel N, Middeke JM, Schetelig J, Bornhäuser M. Prevention and treatment of tumor lysis syndrome, and the efficacy and role of rasburicase. *Onco Targets Ther*. **2017;10**:597. doi: 10.2147/OTT.S103864.
7. Lopez-Olivo MA, Pratt G, Palla SL, Salahudeen A. Rasburicase in tumor lysis syndrome of the adult: a systematic review and meta-analysis. *Am J Kidney Dis*. **2013;62**(3):481-92. doi: 10.1053/j.ajkd.2013.02.378.
8. Retailleau P, Colloc'h N, Vivarès D, Bonnete F, Castro B, El Hajji M, et al. Complexed and ligand-free high-resolution structures of urate oxidase (Uox) from Aspergillus flavus: a reassignment of the active-site binding mode. *Acta Crystallogr., Sect. D: Biol Crystallogr*. **2004;60**(3):453-62. doi: 10.1107/S0907444903029718.
9. Gabison L, Chiadmi M, El Hajji M, Castro B, Colloc'h N, Prangé T. Near-atomic resolution structures of urate oxidase complexed with its substrate and analogues: the protonation state of the ligand. *Acta Crystallogr., Sect. D: Biol Crystallogr*. **2010;66**(6):714-24. doi: 10.1107/S090744491001142X.
10. Retailleau P, Colloc'h N, Vivares D, Bonneté F, Castro B, El Hajji M, et al. Urate oxidase from Aspergillus flavus: new crystal-packing contacts in relation to the content of the active site. *Acta Crystallogr., Sect. D: Biol Crystallogr*. **2005;61**(3):218-29. doi: 10.1107/S0907444904031531.
11. Legoux R, Delpech B, Dumont X, Guillemot JC, Ramond P, Shire D, et al. Cloning and expression in Escherichia coli of the gene encoding Aspergillus flavus urate oxidase. *J Biol Chem.* **1992;267**(12):8565-70.
12. Fazel R, Zarei N, Ghaemi N, Namvaran MM, Enayati S, Ardakani EM, et al. Cloning and expression of Aspergillus flavus urate oxidase in Pichia pastoris. *Springer Plus*. **2014;3**(1):395. doi: 10.1186/2193-1801-3-395.
13. Li J, Chen Z, Hou L, Fan H, Weng S, Xu Ce, et al. High-level expression, purification, and characterization of non-tagged Aspergillus flavus urate oxidase in Escherichia coli. *Protein Expression Purif*. **2006;49**(1):55-9. doi: 10.1016/j.pep.2006.02.003.
14. Azizi M, Enayati S, Salmasizadeh M, Khalaj V. Cloning, Expression, and Purification of Recombinant Urate Oxidase Using Intein Sequence and Elastin-like Protein. *Pathobiol Res*. **2018;21**(1):7-13.
15. Meraj M, Javed S, Shaikh S-U-D, Khaskhili S, Irfan R. Kinetic and Thermodynamic Properties of Purified Wild and Mutant Derived Urate Oxidase. *Curr Sci*. **2017;114**: n. pag.
16. Privalov PL, Gill SJ. Stability of protein structure and hydrophobic interaction. *Adv Protein Chem*. **1988;39**:191-234. doi: 10.1016/s0065-3233(08)60377-0.
17. Imani M, Hosseinkhani S, Ahmadian S, Nazari M. Design and introduction of a disulfide bridge in firefly luciferase: increase of thermostability and decrease of pH sensitivity. *Photochem Photobiol Sci.* **2010;9**(8):1167-77. doi: 10.1039/C0PP00105H.
18. Li W, Xu S, Zhang B, Zhu Y, Hua Y, Kong X, et al. Directed evolution to improve the catalytic efficiency of urate oxidase from Bacillus subtilis. *PLosONE*. **2017;12**(5):e0177877. doi: 10.1371/journal.pone.0177877.
19. Hibi T, Kume A, Kawamura A, Itoh T, Fukada H, Nishiya Y. Hyperstabilization of Tetrameric Bacillus sp. TB-90 Urate Oxidase by Introducing Disulfide Bonds through Structural Plasticity. *Biochemistry*. **2016;55**(4):724-32. doi: 10.1021/acs.biochem.5b01119.
20. Ansorge W. Next-generation DNA sequencing techniques. *New Biotechnol*. **2009;25**(4):195-203. doi: 10.1016/j.nbt.2008.12.009.
21. Imani M, Shahmohamadnejad S. Recombinant production of Aspergillus Flavus uricase and investigation of its thermal stability in the presence of raffinose and lactose. *Biotech*. **2017;7**(3):201. doi: 10.1007/s13205-017-0841-3.
22. Dani VS, Ramakrishnan C, Varadarajan R. MODIP revisited: Re-evaluation and refinement of an automated procedure for modeling of disulfide bonds in proteins. *Protein Eng*. **2003;16**(3):187-93. doi: 10.1093/proeng/gzg024.
23. Thangudu RR, Vinayagam A, Pugalenthi G, Manonmani A, Offmann B, Sowdhamini R. Native and modeled disulfide bonds in proteins: Knowledge-based approaches toward structure prediction of disulfide-rich polypeptides. *Proteins: Struct. Funct Bioinf.* **2005;58**(4):866-79. doi: 10.1002/prot.20369.
24. Craig DB, Dombkowski AA. Disulfide by Design 2.0: a web-based tool for disulfide engineering in proteins. *BMC Bioinf.* **2013;14**(1):346. doi: 10.1186/1471-2105-14-346.
25. Heckman KL, Pease LR. Gene splicing and mutagenesis by PCR-driven overlap extension. *Nat Protoc*. **2007;2**: 924–32. doi: 10.1038/nprot.2007.132.
26. Bradford MM. A rapid and sensitive method for the quantitation of microgram quantities of protein utilizing the principle of protein-dye binding. *Anal Biochem*. **1976;72**(1-2):248-54. doi: 10.1016/0003-2697(76)90527-3.
27. Riener CK, Kada G, Gruber HJ. Quick measurement of protein sulfhydryls with Ellman's reagent and with 4,4′-dithiodipyridine.

*Anal Bioanal Chem*. **2002;373**(4-5):266-76. doi: 10.1007/s00216-002-1347-2.
28. http://www.worthington-biochem.com/up/assay.html.
29. Mahler H, HuBSCHER G, Baum H. Studies on uricase. I. Preparation, purification, and properties of a cuproprotein. *J Biol Chem*. **1955;216**:625-42.
30. Winther JR, Thorpe C. Quantification of Thiols and Disulfides. *Biochimica et biophysica acta*. **2014;1840**(2):838-46. doi: 10.1016/j.bbagen.2013.03.031.
31. Jo BH, Park TY, Park HJ, Yeon YJ, Yoo YJ, Cha HJ. Engineering de novo disulfide bond in bacterial α-type carbonic anhydrase for thermostable carbon sequestration. *Sci Rep.* **2016;6**:29322. doi: 10.1038/srep29322.
32. Prinz WA, Åslund F, Holmgren A, Beckwith J. The role of the thioredoxin and glutaredoxin pathways in reducing protein disulfide bonds in the Escherichia coli cytoplasm. *J Biol Chem*. **1997;272**(25):15661-7. doi: 10.1074/jbc.272.25.15661.
33. Bessette PH, Åslund F, Beckwith J, Georgiou G. Efficient folding of proteins with multiple disulfide bonds in the Escherichia coli cytoplasm. *Proc Natl Acad Sci. U.S.A*. **1999;96**(24):13703-8. doi: 10.1073/pnas.96.24.13703 pmid: 10570136
34. Clarke J, Fersht AR. Engineered disulfide bonds as probes of the folding pathway of barnase: Increasing the stability of proteins against the rate of denaturation. *Biochemistry*. **1993;32**(16):4322-9. doi: 10.1021/bi00067a022.
35. Pace CN, Fu H, Lee Fryar K, Landua J, Trevino SR, Schell D, et al. Contribution of hydrogen bonds to protein stability *Protein Sci*. **2014;23**(5):652-61. doi: 10.1002/pro.2449.
36. Jaliani HZ, Farajnia S, Mohammadi SA, Barzegar A, Talebi S. Engineering and Kinetic Stabilization of the Therapeutic Enzyme Anabeana variabilis Phenylalanine Ammonia Lyase. *Appl. Biochem Biotechnol*. **2013;171**(7):1805-18. doi: 10.1007/s12010-013-0450-5.
37. Zheng J, Yang T, Zhou J, Xu M, Zhang X, Rao Z. Elimination of a free cysteine by creation of a disulfide bond increases the activity and stability of Candida boidinii formate dehydrogenase. *Appl. Environ. Microbiol*. **2017;83**(2):e02624-16. doi: 10.1128/AEM.02624-16.